UDC 621.313 https://doi.org/10.20998/2074-272X.2026.3.09

P.D. Nguyen, M. Kuchar

Performance improvement of sensorless scalar and vector control for induction motor drives via an enhanced voltage model

Introduction. *Scalar control (SC) and field-oriented control (FOC) are widely used in sensorless induction motor (IM) drives for their balance of performance and cost. Among estimation techniques, the voltage-model (VM) based model reference adaptive system (MRAS) is preferred in industry due to its simple structure and low computational load.* ***Problem.*** *Traditional VM-based MRAS schemes are highly sensitive to parameter uncertainties, especially to variations in stator resistance R_s caused by temperature changes. These variations degrade flux estimation accuracy, leading to significant speed-tracking errors, increased transients, and reduced stability in both SC and FOC.* ***Goal.*** *This study quantitatively evaluates how the estimation of stator resistance R_s and the dependent rotor resistance R_r affects the speed-control performance of sensorless SC and FOC under parameter mismatch.* ***Methodology.*** *An improved VM-based MRAS is proposed with parallel R_s estimation and R_r updated via a linear relation to R_s. Estimator stability and convergence are proven using Lyapunov theory. The estimator is integrated into SC and FOC and tested in MATLAB/Simulink under identical conditions, including a sudden 30 % increase in resistance. Speed tracking is quantified using the integral of time-weighted absolute error (ITAE).* ***Results.*** *Parameter estimation markedly enhances the robustness of both strategies. In sensorless SC, ITAE drops by about 66.2 % (5.512 to 1.863), indicating much lower transient oscillations. In sensorless FOC, ITAE falls by about 54 % (0.7075 to 0.323), with speed overshoot nearly eliminated (0.031).* ***Scientific novelty.*** *The study provides a unified quantitative comparison of sensorless SC and FOC using ITAE under identical operating and estimation conditions, revealing different levels of performance recovery with the proposed dual-resistance adaptation.* ***Practical value.*** *The findings guide the design of more reliable industrial IM drives, showing that while FOC retains superior dynamics, SC with estimation becomes a robust, cost-effective option for applications with significant parameter uncertainty.* References 31, table 1, figures 13.

Key words: **induction motor, sensorless control, scalar control, field-oriented control, model reference adaptive system, stator resistance estimation.**

Вступ. *Скалярне керування (SC) та векторне керування (FOC) широко застосовуються в бездатчикових електроприводах з асинхронними двигунами (IM) завдяки оптимальному поєднанню ефективності та вартості. Серед методів оцінювання адаптивна система з еталонною моделлю (MRAS) на основі моделі напруги (VM) є поширеною в промисловості завдяки простій структурі та низьким обчислювальним витратам.* ***Проблема***. *Традиційні схеми MRAS на основі моделі напруги є високочутливими до невизначеностей параметрів, особливо до змін опору статора (R_s), спричинених температурними впливами. Такі зміни погіршують точність оцінювання потокозчеплення, що призводить до значних похибок відстеження швидкості, зростання перехідних процесів і зниження стійкості як у SC, так і у FOC.* ***Мета***. *Кількісно оцінити вплив оцінювання опору статора R_s та пов'язаного з ним опору ротора R_r на характеристики керування швидкістю в бездатчикових системах SC і FOC за умов розузгодження параметрів.* ***Методика***. *Запропоновано вдосконалену систему MRAS на основі моделі напруги з паралельним оцінюванням R_s та оновленням R_r за лінійною залежністю від R_s. Стійкість і збіжність оцінювача доведено з використанням теорії Ляпунова. Оцінювач інтегровано до структур SC і FOC та досліджено в середовищі MATLAB/Simulink за однакових умов, зокрема при раптовому збільшенні опору на 30 %. Якість відстеження швидкості оцінювалася за інтегральним критерієм абсолютної похибки, зваженої за часом (ITAE).* ***Результати***. *Оцінювання параметрів суттєво підвищує робастність обох стратегій. Для бездатчикового SC значення ITAE зменшилося приблизно на 66,2 % (з 5,512 до 1,863), що свідчить про істотне зниження перехідних коливань. Для бездатчикового FOC значення ITAE знизилося приблизно на 54 % (з 0,7075 до 0,323), при цьому перерегулювання швидкості було майже повністю усунено (0,031).* ***Наукова новизна***. *У роботі наведено уніфіковане кількісне порівняння бездатчикових систем SC і FOC за критерієм ITAE в однакових умовах роботи та оцінювання, що дозволило виявити різний рівень відновлення характеристик при запропонованій адаптації двох опорів.* ***Практична значимість***. *Отримані результати можуть бути використані під час проєктування більш надійних промислових електроприводів з асинхронними двигунами. Показано, що хоча FOC зберігає перевагу за динамічними характеристиками, SC з оцінюванням параметрів є робастним і економічно доцільним рішенням для застосувань зі значною невизначеністю параметрів.* Бібл. 31, табл. 1, рис. 13.

Ключові слова: **асинхронний двигун, бездатчикове керування, скалярне керування, векторне керування, адаптивна система з еталонною моделлю, оцінювання опору статора.**

Introduction. The induction motors (IMs) is widely used in variable-speed drive systems due to its simple structure, low production cost, and high operational reliability [1, 2]. Their favorable efficiency, low acoustic noise, and limited maintenance requirements have led to extensive adoption in pumps, compressors, conveyor systems, ventilation units, automated production lines, and various mechatronic applications. To control IM drives, several strategies are commonly employed, including scalar control (SC) based on the voltage-frequency (V/f) relationship [3-8] and field-oriented control (FOC) [9-11]. Among these methods, FOC is particularly suitable for applications requiring fast dynamic response, as they decouple torque and flux components through coordinate transformations, enabling independent regulation of these variables. Consequently, FOC is generally regarded as the preferred solution for high-performance IM drives [12-14].

Problems and the relevance. Although modern control techniques have significantly evolved, SC remains widely adopted in industrial practice due to its low implementation cost and structural simplicity. Classical V/f-based SC schemes maintain an approximately constant stator flux by preserving a fixed voltage-frequency ratio [15, 16]. However, it has been well documented that such an approach exhibits limited capability in handling dynamic operating conditions, particularly during load disturbances and rapid speed variations, with performance degradation becoming more evident in sensorless (SSL) operation. Comparative investigations indicate that while closed-loop SC schemes enhance performance relative to open-loop implementations, they still fall short of vector control methods in terms of dynamic response and speed regulation accuracy [17]. This trade-off between performance and simplicity highlights the need to improve the operating characteristics of different control strategies, particularly in SSL configurations.

Review of recent publications on SSL control of IM drives. SSL control for IM drives is gaining attention because it reduces hardware costs and improves reliability

by eliminating mechanical speed sensors [18-20]. Traditional observer-based methods, such as sliding mode observers, remain widely used for their robustness to noise and parameter deviations and can provide acceptable speed estimation under load variations, though low-speed performance and vibration issues persist [21]. AI-based methods and hybrid observer-machine learning schemes demonstrate that AI-assisted sensorless IM control with dual magnetic-field orientation improves speed estimation accuracy and robustness to parameter variations compared with traditional approaches [22]. The work [23] shows that combining an extended Kalman filter (EKF) with a neural network-based magnetic model significantly enhances speed estimation and stability in electric drives, offering useful guidance for sensorless IM systems.

Model reference adaptive systems (MRAS) are widely used for SSL control because they have moderate computational complexity and integrate easily into traditional control structures. They estimate rotor speed by minimizing the difference between a reference model and an adaptive model, typically based on a voltage model (VM) or current model, making them suitable for real-time industrial use [24, 25]. Sensorless control with MRAS offers a good trade-off between estimation accuracy, robustness, and cost compared to more complex AI-based or EKF methods. However, traditional MRAS is sensitive to parameter deviations, especially R_s variations at low speed, motivating advanced MRAS designs with parameter adaptation to improve stability and robustness under changing operating conditions [26].

The goal of the paper. This study quantitatively evaluates how the estimation of stator resistance R_s and the dependent rotor resistance R_r affects the speed-control performance of sensorless SC and FOC under parameter mismatch. An improved VM-based MRAS with parallel resistance estimation is embedded in both schemes under identical conditions, using the integral of time-weighted absolute error (ITAE) index [27] for a unified assessment of speed tracking accuracy and robustness.

Mathematical model of the IM. In the stationary (α, β) frame, the dynamic behavior of an IM is described by voltage and flux-linkage equations, which relate the stator currents, rotor flux components, and motor parameters, as described as:

$$\boldsymbol{u}_s^s = R_s \boldsymbol{i}_s^s + \frac{\mathrm{d}\boldsymbol{\psi}_s^s}{\mathrm{d}t}; \quad (1)$$

$$0 = R_r \boldsymbol{i}_r^s + \frac{\mathrm{d}\boldsymbol{\psi}_r^s}{\mathrm{d}t} - j\omega_r \boldsymbol{\psi}_r^s; \quad (2)$$

$$\boldsymbol{\psi}_s^s = L_s \boldsymbol{i}_s^s + L_m \boldsymbol{i}_r^s; \quad (3)$$

$$\boldsymbol{\psi}_r^s = L_m \boldsymbol{i}_s^s + L_r \boldsymbol{i}_r^s; \quad (4)$$

where $\boldsymbol{i}_s^s$, $\boldsymbol{i}_r^s$ are the stator and rotor current vectors; $\boldsymbol{u}_s^s$, $\boldsymbol{u}_r^s$ are the stator and rotor voltage vectors; $\boldsymbol{\psi}_s^s$, $\boldsymbol{\psi}_r^s$ are the stator and rotor flux-linkage vectors; R_s, R_r are the stator and rotor resistances; L_s, L_r, L_m are the stator, rotor and magnetizing inductances; ω_r is the electrical angular speed; T_e is the electromagnetic torque.

By combining (1)-(4), the electromagnetic torque T_e is obtained as:

$$T_e = \frac{3}{2} p L_m \operatorname{Im}\left\{\boldsymbol{i}_s^s, \boldsymbol{\psi}_r^s\right\}, \quad (5)$$

where p is the number of pairs of poles.

SSL control for IM drive. The proposed SSL employs an improved MRAS scheme for rotor speed estimation. The observer compares the rotor flux obtained from the VM-based reference model with that generated by the adaptive model (AM). The resulting flux error is processed by an adaptive PI mechanism to update the estimated quantities. As shown in Fig. 1, the proposed MRAS structure incorporates parallel estimation of the R_s and rotor time constant (T_r) together with the rotor speed. Compared with conventional VM-based MRAS approaches, this enhanced structure improves robustness against parameter variations and changes in operating conditions.

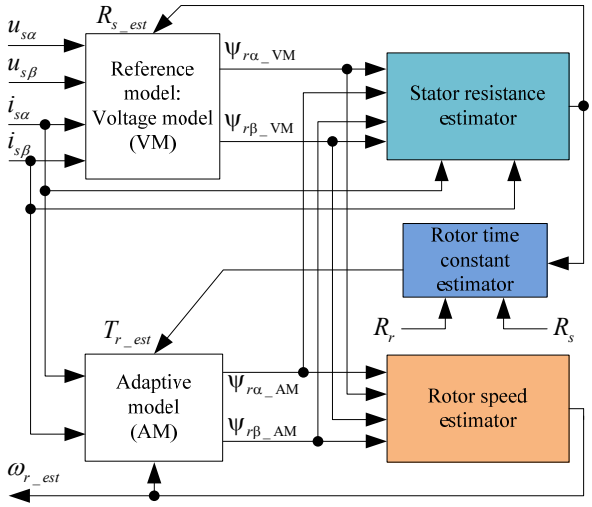

Fig. 1. Sensorless speed based on improved MRAS using VM

Reference model using VM. In the stationary (α, β) frame, the rotor flux components of the VM are expressed via the IM voltage equations:

$$\psi_{r\alpha\_VM} = \frac{L_r}{L_m}\left[\int\left(u_{s\alpha} - R_{s\_est} i_{s\alpha}\right)\mathrm{d}t - \frac{L_s L_r - L_m^2}{L_r} i_{s\alpha}\right]; \quad (6)$$

$$\psi_{r\beta\_VM} = \frac{L_r}{L_m}\left[\int\left(u_{s\beta} - R_{s\_est} i_{s\beta}\right)\mathrm{d}t - \frac{L_s L_r - L_m^2}{L_r} i_{s\beta}\right], \quad (7)$$

where $\psi_{r\alpha\_VM}$, $\psi_{r\beta\_VM}$ are the rotor flux components from VM; R_{s_est} is the estimated R_s.

Based on the rotor flux components in (6), (7), the rotor flux angle (γ_r) is computed by:

$$\gamma_r = \tan^{-1}\left(\frac{\psi_{r\beta\_VM}}{\psi_{r\alpha\_VM}}\right). \quad (8)$$

Adaptive model and rotor speed estimation. The rotor flux in the AM is computed from the estimated speed and stator current dynamics, as follows:

$$\frac{\mathrm{d}\psi_{r\alpha\_AM}}{\mathrm{d}t} = \frac{L_m}{T_{r\_est}} i_{s\alpha} - \frac{1}{T_{r\_est}}\psi_{r\alpha\_AM} - \omega_{r\_est}\psi_{r\beta\_AM}; \quad (9)$$

$$\frac{\mathrm{d}\psi_{r\beta\_AM}}{\mathrm{d}t} = \frac{L_m}{T_{r\_est}} i_{s\beta} - \frac{1}{T_{r\_est}}\psi_{r\beta\_AM} + \omega_{r\_est}\psi_{r\alpha\_AM}. \quad (10)$$

The estimated rotor speed is obtained via an adaptive PI mechanism:

$$\varepsilon_\omega = \psi_{r\alpha\_AM}\psi_{r\beta\_VM} - \psi_{r\alpha\_VM}\psi_{r\beta\_AM}; \quad (11)$$

$$\omega_{r\_est} = K_{p\omega}\varepsilon_\omega + K_{i\omega}\int \varepsilon_\omega \mathrm{d}t; \quad (12)$$

where $\psi_{r\alpha\_AM}$, $\psi_{r\beta\_AM}$ are the rotor flux components from AM; T_{r_est} is the estimated rotor time constant; ε_ω is the flux

error function used as the adaptation signal; ω_{r_est} is the estimated rotor speed; $K_{p\omega}$, $K_{i\omega}$ are the proportional and integral gains of the adaptive PI controller.

Parameter identification for the improved structure. In SSL systems for IM drives, the precision of the estimated rotor speed is highly dependent on the stability and accuracy of the motor parameters. To overcome inaccuracies caused by parameter variations during operation, this study performs parallel estimation of the R_s and T_r to ensure the convergence and reliability of the improved MRAS.

Variations in R_s directly affect the accuracy of the rotor flux calculated in the VM through (6), (7). Therefore, R_s estimation is performed in parallel with the speed estimation process to account for these changes. A PI controller is used to estimate the stator resistance as:

$$\varepsilon_R = i_{s\alpha}\left(\psi_{r\alpha\_VM} - \psi_{r\alpha\_AM}\right) + i_{s\beta}\left(\psi_{r\beta\_VM} - \psi_{r\beta\_AM}\right); \quad (13)$$

$$R_{s\_est} = K_{pR}\varepsilon_R + K_{iR}\int \varepsilon_R \mathrm{d}t, \quad (14)$$

where K_{pR}, K_{iR} denote the PI controller parameters for R_s estimation, respectively.

The rotor time constant is a core parameter in the AM, as seen in (9), (10). However, T_r cannot be directly measured and is difficult for standard observers to identify independently. To address this limitation, this research uses a method, in which R_r is linearly adjusted relative to the estimated R_s:

$$R_{r\_est} = \frac{R_{s\_est}}{R_s} R_r. \quad (15)$$

Under the assumption that the ratio L_r/R_r remains weakly affected by temperature variations relative to R_s, T_r can be treated as quasiconstant during the estimation process:

$$T_{r\_est} = \frac{L_r}{R_{r\_est}}. \quad (16)$$

Stability analysis of the estimation observer using Lyapunov theory. To guarantee bounded estimation errors and convergence of the adaptive scheme to the true values, the stability of the proposed MRAS observer is analyzed via Lyapunov stability theory [28, 29].

Let the state error vector be defined as $\boldsymbol{\varepsilon} = \boldsymbol{\psi}^S_{r\_CM} - \boldsymbol{\psi}^S_{r\_VM}$. We define the parameter estimation errors as $\Delta\omega_r = \omega_r - \omega_{r\_est}$ and $\Delta R_s = R_s - R_{s\_est}$.

To ensure the simultaneous stability of the flux observer and the parameter estimators, a quadratic Lyapunov candidate function V is defined as:

$$V = \frac{1}{2}\boldsymbol{\varepsilon}^T\boldsymbol{\varepsilon} + \frac{1}{2\lambda_1}(\Delta\omega_r)^2 + \frac{1}{2\lambda_2}(\Delta R_s)^2, \quad (17)$$

where λ_1, λ_2 are the positive constants representing the adaptation gains. The function V is positive definite ($V>0$) for all non-zero errors and equals zero only when the estimated states and parameters match the actual values.

The time derivative of the Lyapunov function is given by:

$$\frac{\mathrm{d}V}{\mathrm{d}t} = \boldsymbol{\varepsilon}^T\frac{\mathrm{d}\boldsymbol{\varepsilon}}{\mathrm{d}t} - \frac{1}{\lambda_1}\Delta\omega_r\frac{\mathrm{d}\omega_{r\_est}}{\mathrm{d}t} - \frac{1}{\lambda_2}\Delta R_s\frac{\mathrm{d}R_{s\_est}}{\mathrm{d}t} \quad (18)$$

with λ_1, λ_2 are the positive constants that ensure the positive definiteness of V.

Based on the error dynamics of the improved MRAS derived from (11)-(14), the term $\boldsymbol{\varepsilon}^T(\mathrm{d}\boldsymbol{\varepsilon}/\mathrm{d}t)$ contains components related to the parameter mismatches. To ensure asymptotic stability $\mathrm{d}V/\mathrm{d}t$, the adaptation mechanisms must be chosen to cancel out the indefinite terms in the derivative.

By equating the parameter update rates to the error driving terms, we derive the following adaptation laws:

For rotor speed in (12): the adaptation law minimizes the cross-product of the flux error, which corresponds to the torque error component. This satisfies the condition for minimizing the $\Delta\omega_r$ term in the Lyapunov derivative.

For R_s in (14): the adaptation law is proportional to the dot-product of the stator current and the flux error, representing the resistive voltage drop error.

The PI controllers are employed for both the speed estimator and the R_s estimator [30]. For the speed estimation loop, a parallel PI structure is adopted with gains $K_{p\omega}$=150, $K_{i\omega}$=1500. For the R_s estimation loop, a parallel PI controller with gains K_{pR}=3.6, K_{iR}=12 is implemented. These gains are tuned to achieve smooth tracking of the R_s while minimizing its interaction with the speed estimation loop.

Improved closed-loop SC. The main principle of the closed-loop SC method is to use an estimated speed technique to calculate slip compensation [31]. Figure 2 shows the control structure of the closed-loop SC with slip compensation using improved MRAS.

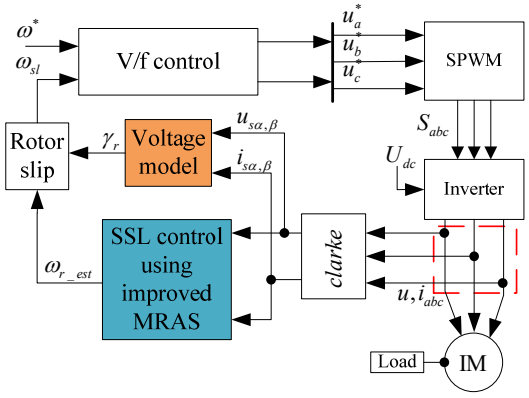

Fig. 2. Block diagram of the SC using SSL

In this structure, the γ_r in (8) is used to compute the slip frequency, which is fed back to correct the commanded synchronous frequency, thereby improving speed regulation and transient performance. The synchronous speed of the rotor flux ω_s is determined by differentiating γ_r and the slip frequency ω_{sl} is defined as:

$$\omega_s = \mathrm{d}\gamma_r/\mathrm{d}t; \quad (19)$$

$$\omega_{sl} = \left(\omega_s - \omega_{r\_est}\right)/p. \quad (20)$$

Improved FOC control. FOC is a widely adopted vector control technique for IM drives requiring fast dynamic response. By orienting the rotating reference frame along the rotor flux, the stator current vector is separated into orthogonal components associated with flux production and torque generation, enabling independent control of these quantities.

Reliable FOC operation depends on accurate information about the γ_r and rotor speed. To eliminate mechanical sensors, an improved FOC structure based on SSL is employed [10, 11]. The overall configuration of FOC using improved MRAS is illustrated in Fig. 3.

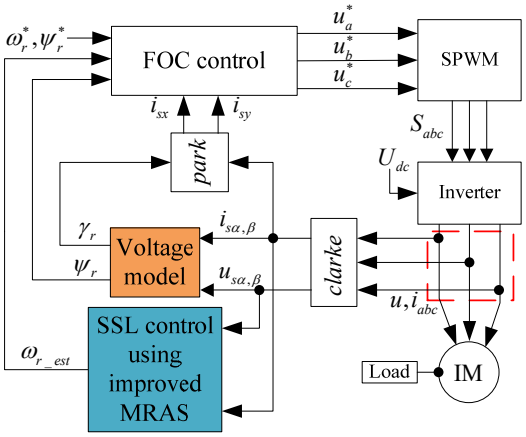

Fig. 3. Block diagram of the IM drive using SSL

Performance evaluation criteria. The performance of each control scheme is evaluated using the ITAE index [7, 27]. By weighting the tracking error with time, the ITAE criterion effectively reflects prolonged deviations between the actual and reference signals. The index is calculated over a 5 s interval as:

$$ITAE = \int_0^T t\left|\left(\omega_m - \omega_m^*\right)\right| \mathrm{d}t \,, \qquad (21)$$

where ω_m, ω_m^* are the real and reference mechanical angular speeds of the IM, respectively.

Simulation results. To validate the proposed MRAS-based SSL scheme with integrated R_s and R_r estimation, an IM drive was simulated under SC and FOC. The goal was to assess how resistance estimation affects speed control performance for both strategies under identical conditions.

In all simulations, the reference speed increased linearly from 0 to 710 rpm at 0.5 s, with a constant 1 N·m load torque applied from startup. Two cases are considered to assess the impact of R_s and R_r estimation:

Case 1: No R_s and R_r estimation.

Case 2: Estimation of both R_s and R_r.

The IM parameters are as follows: $p = 2$; rated speed 1420 rpm; $R_s = 3.179$ Ω; $R_r = 2.118$ Ω; $L_s = 0.209$ H; $L_r = 0.209$ H; $L_m = 0.192$ H.

A. Sensorless SC. In the sensorless SC scheme without resistance adaptation, the controller uses fixed nominal R_s and R_r while the actual motor parameters vary. As shown in Fig. 4, the deviation between nominal and actual resistances increases over time, distorting the torque-speed relationship and causing oscillatory transients and poorer tracking, as seen in the rotor speed response in Fig. 5. This demonstrates that sensorless SC is highly sensitive to parameter variations without estimation.

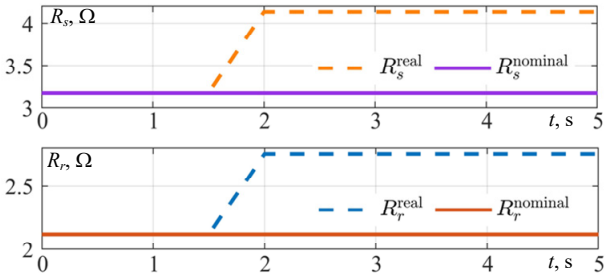

Fig. 4. Actual and nominal R_s/R_r under SC without resistance estimation

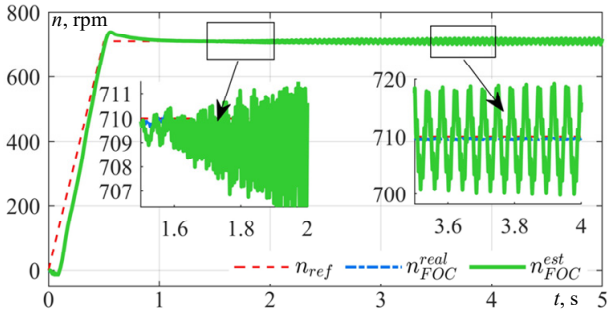

Fig. 5. Rotor speed response under sensorless SC without R_s/R_r estimation (reference, real and estimated)

With the proposed resistance estimation, the estimated R_s and R_r closely match their actual values (Fig. 6). The estimation errors converge quickly and remain bounded (Fig. 7). The improved parameter accuracy yields a much smoother rotor speed response with reduced oscillations and better tracking (Fig. 8). The performance indices in Table 1 confirm that the estimation scheme significantly improves the transient response and robustness of sensorless SC under varying operating conditions.

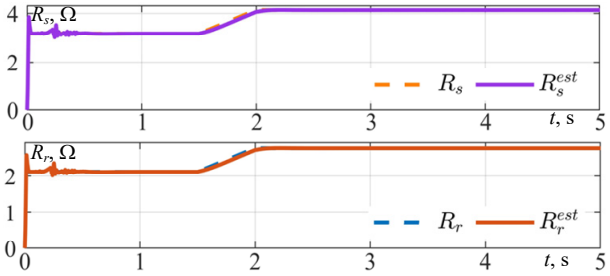

Fig. 6 Actual and estimated R_s/R_r under sensorless SC

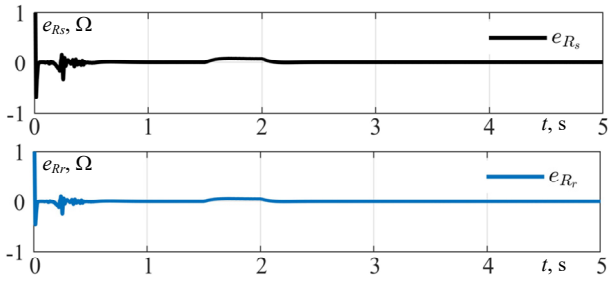

Fig. 7. Estimation errors of R_s/R_r under sensorless SC

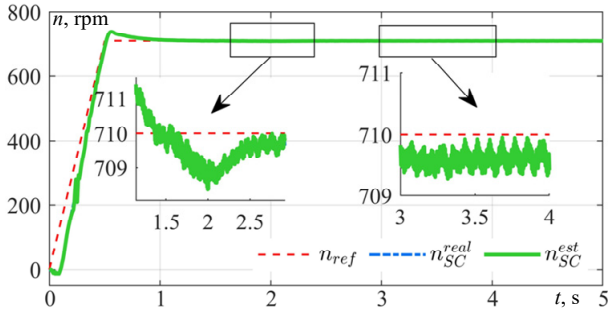

Fig. 8. Rotor speed response under sensorless SC with R_s/R_r estimation (reference, real and estimated)

B. Sensorless FOC. In sensorless FOC without resistance estimation, the R_s and R_r in the controller and MRAS observer are kept constant, while the actual R_s increases during operation (Fig. 9). This mismatch degrades rotor flux and adaptive speed estimation, causing the rotor speed response in Fig. 10 to show large transients and poor tracking, highlighting the sensitivity of sensorless FOC to resistance mismatches without adaptation.

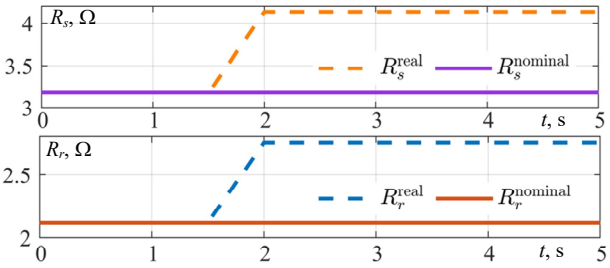

Fig. 9. Actual and nominal R_s/R_r under parameter variation

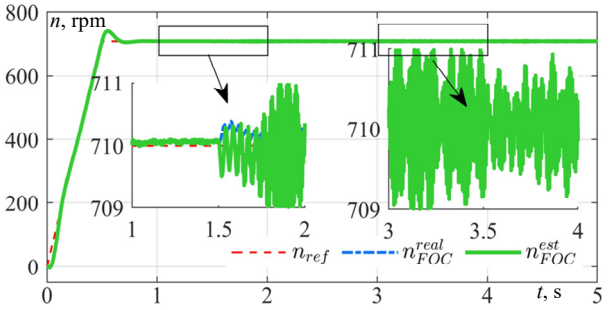

Fig. 10. Rotor speed response without R_s/R_r estimation (reference, real and estimated)

With the proposed MRAS-based resistance estimation enabled, R_s and R_r are accurately identified (Fig. 11). The estimation errors converge rapidly (Fig. 12). This improved parameter estimation yields more accurate flux and speed estimates, producing a smooth rotor speed response with minimal oscillations (Fig. 13).

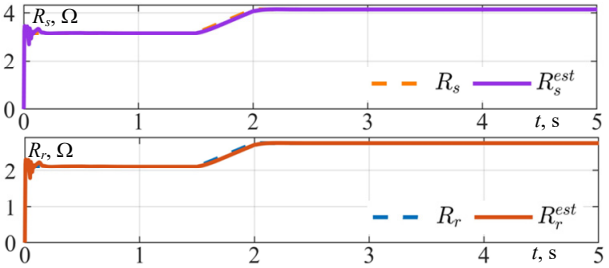

Fig. 11. Actual and estimated R_s/R_r with MRAS-based estimation

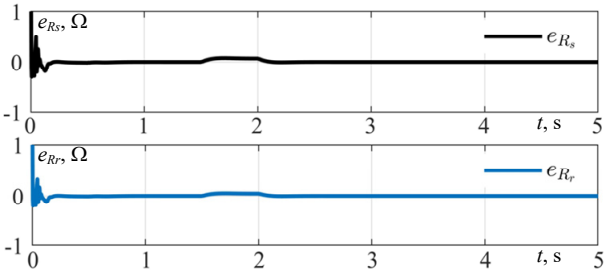

Fig. 12. Estimation errors of R_s/R_r

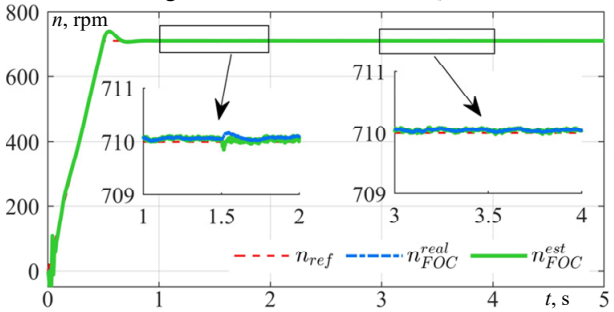

Fig. 13. Rotor speed response with R_s/R_r resistance estimation (reference, real and estimated)

The quantitative results in Table 1 show reduced cumulative tracking error and transient deviations, confirming the method's effectiveness in enhancing the dynamic behavior and robustness of sensorless FOC.

C. Quantitative performance comparison. Table 1 summarizes the speed performance of sensorless SC and FOC with and without resistance estimation. For both methods, ignoring resistance variations severely degrades performance under parameter uncertainties, whereas the proposed estimation consistently improves tracking and reduces transients. Sensorless FOC still outperforms SC dynamically due to its decoupled structure. Still, both benefit markedly from the MRAS-based resistance estimation, which mitigates parameter mismatch and improves the reliability of sensorless IM drives under variable conditions.

Table 1

Speed performance comparison under SC and FOC

Control strategy	R_s/R_r estimation	Speed ITAE	Speed overshoot	Performance assessment
SC	No	5.512	7.895	Large oscillations, low robustness
	Yes	1.863	0.0196	Better tracking, higher robustness
FOC	No	0.7075	0.2987	Large transient deviation
	Yes	0.3230	0.0310	Smooth response, high robustness

Conclusion. This paper examined how estimation of R_s and R_r resistances affects sensorless IM drives using SC and FOC. An improved MRAS-based scheme with parallel resistance updates was proposed to reduce parameter mismatch effects.

Without estimation, both strategies degraded under resistance variations. In sensorless SC, the mismatch caused significant tracking errors (ITAE 5.512) and high overshoot (7.895). With estimation enabled, ITAE fell to 1.863 and overshoot to 0.0196, significantly improving steady-state and transient performance.

In sensorless FOC, baseline performance was better (ITAE 0.7075), but resistance changes still induced transient deviations (overshoot 0.2987). Estimation reduced the overshoot to 0.0310 and the ITAE to 0.3230, further enhancing the dynamics.

Thus, although FOC remains dynamically superior, both strategies gain substantially from the proposed MRAS-based resistance estimation, with SC significantly narrowing the gap. Resistance estimation is therefore crucial for robustness, reduced transients, and reliable sensorless IM operation under parameter uncertainties.

The results demonstrate the performance gains of the proposed estimator and provide practical guidance for a robust, cost-effective solution under parameter uncertainty.

In the future, it is necessary to conduct real IM drives experimental studies of examined how estimation of R_s and R_r resistances affects sensorless IM drives using SC and FOC based on proposed an improved MRAS-based scheme with parallel resistance updates to reduce parameter mismatch effects.

Acknowledgment. This work is a part of the research project [CS.2025.B1.023] funded by Saigon University.

Conflict of interest. The authors declare that they have no conflicts of interest.

REFERENCES

1. Ibrar A., Ahmad S., Safdar A., Haroon N. Efficiency enhancement strategy implementation in hybrid electric vehicles using sliding mode control. *Electrical Engineering & Electromechanics*, 2023, no. 1, pp. 10-19. doi: https://doi.org/10.20998/2074-272X.2023.1.02.

2. Tiwari D., Miscandlon J., Tiwari A., Jewell G.W. A Review of Circular Economy Research for Electric Motors and the Role of Industry 4.0 Technologies. *Sustainability*, 2021, vol. 13, no. 17, art. no. 9668. doi: https://doi.org/10.3390/su13179668.
3. Liyanage A., Nagrial M., Hellany A., Rizk J. Speed Control of Induction Motors Using V/f Control Method. *2022 International Conference on Electrical and Computing Technologies and Applications (ICECTA)*, 2022, pp. 424-429. doi: https://doi.org/10.1109/ICECTA57148.2022.9990374.
4. Saleh S.A. The Development and Performance Testing of a V/f Control for Induction Motors Fed by Wavelet Modulated Power Electronic Converters. *IEEE Transactions on Industry Applications*, 2024, vol. 60, no. 3, pp. 5012-5024. doi: https://doi.org/10.1109/TIA.2024.3362918.
5. Keskin B., Eminoglu I. Optimally Tuned PI Controller Design for V/f Control of Induction Motor. *2022 International Congress on Human-Computer Interaction, Optimization and Robotic Applications (HORA)*, 2022, pp. 1-5. doi: https://doi.org/10.1109/HORA55278.2022.9800005.
6. Son D.-H., Kim S.-A. Simplified V/f Control Algorithm for Reduction of Current Fluctuations in Variable-Speed Operation of Induction Motors. *Energies*, 2024, vol. 17, no. 7, art. no. 1699. doi: https://doi.org/10.3390/en17071699.
7. Shekher V., Sisodiya A., Sinha A.K., Harsh H., Soren N. Optimal tuning of PID controller for V/f control of linear induction motor using artificial biological intelligence. *Franklin Open*, 2024, vol. 9, art. no. 100183. doi: https://doi.org/10.1016/j.fraope.2024.100183.
8. Choi S.-C., Kim J.-H., Yoon Y.-D., Hong C.-O., Park C.-H., Cho J.-H. V/F Control Method for Pulsating Torque Reduction in a Single Phase Induction Motor. *2023 IEEE International Symposium on Sensorless Control for Electrical Drives (SLED)*, 2023, pp. 1-6. doi: https://doi.org/10.1109/SLED57582.2023.10261379.
9. Zellouma D., Bekakra Y., Benbouhenni H. Field-oriented control based on parallel proportional–integral controllers of induction motor drive. *Energy Reports*, 2023, vol. 9, pp. 4846-4860. doi: https://doi.org/10.1016/j.egyr.2023.04.008.
10. Tran C.D., Kuchar M., Nguyen P.D. Improved Rotor Flux Estimation For Field-Oriented Control In Induction Motor Drives. *Tekhnichna Elektrodynamika*, 2025, no. 6, pp. 52-57. doi: https://doi.org/10.15407/techned2025.06.052.
11. Tran C.D., Kuchar M., Sotola V., Nguyen P.D. Sensor fault diagnosis strategy based on rotor flux observers in three-phase induction motor drive. *Scientific Reports*, 2025, vol. 16, no. 1, art. no. 267. doi: https://doi.org/10.1038/s41598-025-29381-9.
12. Soliman H.M. Studying the Steady State Performance Characteristics of Induction Motor with Field Oriented Control Comparing to Scalar Control. *European Journal of Engineering and Technology Research*, 2018, vol. 1, no. 2, pp. 18-25. doi: https://doi.org/10.24018/ejeng.2016.1.2.115.
13. Bierhoff M., Busch J. Novel Scalar versus Field Oriented Speed Control of Induction Machine Drives. *2020 International Symposium on Power Electronics, Electrical Drives, Automation and Motion (SPEEDAM)*, 2020, pp. 207-212. doi: https://doi.org/10.1109/SPEEDAM48782.2020.9161939.
14. Rezgui S.E., Darsouni Z., Benalla H. Nonlinear vector control of multiphase induction motor using linear quadratic regulator and active disturbances rejection control under disturbances and parameter variations. *Electrical Engineering & Electromechanics*, 2025, no. 6, pp. 75-83. doi: https://doi.org/10.20998/2074-272X.2025.6.10.
15. Graciola C.L., Goedtel A., Angélico B.A., Castoldi M.F., Costa B.L.G. Energy Efficiency Optimization Strategy for Scalar Control of Three-Phase Induction Motors. *Journal of Control, Automation and Electrical Systems*, 2022, vol. 33, no. 3, pp. 1032-1043. doi: https://doi.org/10.1007/s40313-021-00876-w.
16. Laha S., Dhali J., Gayen P.K. Comparative Performance between V/F and Rotor Flux-Oriented Controls of Induction Motor Drive. *2023 IEEE Devices for Integrated Circuit (DevIC)*, 2023, pp. 1-6. doi: https://doi.org/10.1109/DevIC57758.2023.10134999.
17. Bisoi M., Kalyan R., Selvaraj R., Vemuganti H.P. Performance investigation of three-phase induction machine with scalar and vector control method. *Emerging Technologies & Applications in Electrical Engineering*, 2024, pp. 152-162. doi: https://doi.org/10.1201/9781003505181-19.
18. Gholipour A., Ghanbari M., Alibeiki E., Jannati M. Speed sensorless fault-tolerant control of induction motor drives against current sensor fault. *Electrical Engineering*, 2021, vol. 103, no. 3, pp. 1493-1513. doi: https://doi.org/10.1007/s00202-020-01179-0.
19. Tran C.D., Kuchar M., Nguyen P.D. Research for an enhanced fault-tolerant solution against the current sensor fault types in induction motor drives. *Electrical Engineering & Electromechanics*, 2024, no. 6, pp. 27-32. doi: https://doi.org/10.20998/2074-272X.2024.6.04.
20. Wogi L., Morawiec M., Ayana T. Sensorless Control of Induction Motor Based on Super-Twisting Sliding Mode Observer With Speed Convergence Improvement. *IEEE Access*, 2024, vol. 12, pp. 74239-74250. doi: https://doi.org/10.1109/ACCESS.2024.3404040.
21. Najeeb M.M., Vidya M.S. Sensorless Speed Control of Induction Motor Using SMO. *2025 International Conference on Power, Instrumentation, Control, and Computing (PICC)*, 2025, pp. 1-5. doi: https://doi.org/10.1109/PICC67314.2025.11291483.
22. Szoke E., Szabo C., Pintilie L.-N. Artificial Intelligence-Based Sensorless Control of Induction Motors with Dual-Field Orientation. *Applied Sciences*, 2025, vol. 15, no. 16, art. no. 8919. doi: https://doi.org/10.3390/app15168919.
23. Pasqualotto D., Rigon S., Zigliotto M. Sensorless Speed Control of Synchronous Reluctance Motor Drives Based on Extended Kalman Filter and Neural Magnetic Model. *IEEE Transactions on Industrial Electronics*, 2023, vol. 70, no. 2, pp. 1321-1330. doi: https://doi.org/10.1109/TIE.2022.3159962.
24. Ganjewar S.P., Pahariya Y. Modified MRAS approach for sensorless speed control of induction motor for reliability improvement. *International Journal of Information Technology*, 2022, vol. 14, no. 3, pp. 1595-1602. doi: https://doi.org/10.1007/s41870-021-00847-z.
25. Orlowska-Kowalska T., Korzonek M., Tarchala G. Performance Analysis of Speed-Sensorless Induction Motor Drive Using Discrete Current-Error Based MRAS Estimators. *Energies*, 2020, vol. 13, no. 10, art. no. 2595. doi: https://doi.org/10.3390/en13102595.
26. Tran C.D., Brandstetter P., Kuchar M., Nguyen P.D. An Improved CB-MRAS Using Voltage Model Integrating Stator Resistance Estimation in Induction Motor Drives. *International Review of Electrical Engineering (IREE)*, 2024, vol. 19, no. 6, art. no. 446. doi: https://doi.org/10.15866/iree.v19i6.25107.
27. Alshatti A.H. An Adaptive Soft Computing Model for Flux Estimation and Torque Control of Induction Motors. *International Journal of Advances in Scientific Research and Engineering*, 2024, vol. 10, no. 5, pp. 1-9. doi: https://doi.org/10.31695/IJASRE.2024.5.1.
28. Gulbudak O., Gokdag M., Komurcugil H. Model Predictive Control Strategy for Induction Motor Drive Using Lyapunov Stability Objective. *IEEE Transactions on Industrial Electronics*, 2022, vol. 69, no. 12, pp. 12119-12128. doi: https://doi.org/10.1109/TIE.2021.3139237.
29. Nurettin A., Inanc N. Sensorless Vector Control for Induction Motor Drive at Very Low and Zero Speeds Based on an Adaptive-Gain Super-Twisting Sliding Mode Observer. *IEEE Journal of Emerging and Selected Topics in Power Electronics*, 2023, vol. 11, no. 4, pp. 4332-4339. doi: https://doi.org/10.1109/JESTPE.2023.3265352.
30. Orlowska-Kowalska T., Dybkowski M. Stator-Current-Based MRAS Estimator for a Wide Range Speed-Sensorless Induction-Motor Drive. *IEEE Transactions on Industrial Electronics*, 2010, vol. 57, no. 4, pp. 1296-1308. doi: https://doi.org/10.1109/TIE.2009.2031134.
31. Meghana I., Cherukupalli K., Sravani M., Babu Naidu P.C. Simulation of Slip Compensation for Induction Motor Drive Using MATLAB. *2021 Innovations in Power and Advanced Computing Technologies (i-PACT)*, 2021, pp. 1-7. doi: https://doi.org/10.1109/i-PACT52855.2021.9696878.

Received 13.01.2026
Accepted 20.03.2026
Published 02.05.2026

P.D. Nguyen[1,2]*, PhD Student,*
M. Kuchar[2]*, Professor, Doctor on Electrical Engineering,*
[1] Faculty of Engineering and Technology,
Saigon University, Ho Chi Minh City, Vietnam,
e-mail: phuong.nd@sgu.edu.vn (Corresponding Author)
[2] Department of Applied Electronics,
Faculty of Electrical Engineering and Computer Science,
VSB-Technical University of Ostrava, Czech Republic.

How to cite this article:
Nguyen P.D., Kuchar M. Performance improvement of sensorless scalar and vector control for induction motor drives via an enhanced voltage model. *Electrical Engineering & Electromechanics*, 2026, no. 3, pp. 62-67. doi: https://doi.org/10.20998/2074-272X.2026.3.09